Geophys. J. Int. (1996) **125**, 857–868

Estimates of stress directions by inversion of earthquake fault-plane solutions in Sicily

D. Caccamo,[1] G. Neri,[1] A. Sarao[2] and M. Wyss[3]

[1] *Dipartimento di Fisica della Materia, Geofisica e Fisica dell 'Ambiente, University of Messina, Italy*

[2] *Istituto di Geodesia e Geofisica, University of Trieste, Italy*

[3] *Geophysical Institute, University of Alaska, Fairbanks, USA*

Accepted 1996 January 25. Received 1996 January 22; in original form 1994 October 28

SUMMARY

The tectonic stress orientation is estimated in the lithosphere of northern Sicily, the southern Tyrrhenian sea and southern Calabria, and in the Wadati–Benioff zone below the Tyrrhenian, by inversion of fault-plane solutions of earthquakes covering a magnitude range from 2.5 to 7.1. Focal mechanisms of 97 earthquakes are taken from the literature, after a critical evaluation of their data quality. An average misfit of $F = 13°$ indicates that the set of all shallow (< 50 km) earthquakes is generated by a heterogeneous stress field. For three subsets, based on regional and magnitude separation, F was small enough ($2.8° \leq F \leq 5.9°$) to support the assumption of a homogeneous stress direction; for an additional subset, with $F = 7.4°$, such a condition is close to being fulfilled even though some heterogeneity appears to be present. The number of earthquakes in these subsets ranged from nine to 22, and the uncertainties of the principal stress directions were generally of the order of 20° at the 90 per cent confidence level. The earthquakes with $M \geq 5$ define a regional stress field with the greatest principal stress, σ_1, dipping at a shallow angle to the south. In north-eastern Sicily and south-western Calabria the stress field estimated by earthquakes is extensional, with σ_3 in a direction of WNW, and a near-vertical σ_1, in agreement with the graben tectonics mapped geologically in this area. In western Sicily the σ_1 direction is oriented WNW, but this result is judged less reliable than the others, based on the broader confidence limits of the solution and the average misfit of 7.4°. The earthquakes in the Wadati–Benioff zone define σ_1 dipping at about 70° to the NW, subparallel to the zone, with σ_2 horizontal and striking parallel to the zone.

Key words: fault-plane solutions, inversion, Italy, stress distribution.

INTRODUCTION

The tectonic setting of the study area is complex. Several microplates, blocks and structural units, possibly derived from the fracturing and consumption of the old margins of the African and Eurasian plates, are present (e.g. Scandone & Patacca 1984). Several tectonic hypotheses have been advanced in the last few decades to explain the structure of the study area, and the debate is apparently far from concluded. For example, it is still uncertain whether, and how, the interaction between the two continental plates influences the local tectonic processes.

The direction of the tectonic stress in the study area is an essential parameter for constructing a tectonic model. Previous analyses of stress have been carried out in the region by Ghisetti (1984), Cristofolini *et al.* (1985), Rebai, Philip & Taboada (1992) and Neri & Wyss (1993). In the first two studies geological data were used. Rebai *et al.* (1992) mapped stress directions on a continental scale for the Mediterranean and Europe, averaging earthquake P- and T-axes, geological data and *in situ* stress measurements. By inverting fault-plane solutions for stress directions, Neri & Wyss (1993) avoided the large uncertainties inherent in the averaging of P- and T-axes (McKenzie 1969), and found stress heterogeneities on a scale of 10 to 50 km in the Southern Tyrrhenian area. In the present study, the inversion algorithm of Gephart & Forsyth (1984) is applied to subsets of a total of 95 fault plane solutions from earthquakes covering the area including western and northern Sicily, the Tyrrhenian sea and southern Calabria. The hypocentral depths ranged from the surface to 360 km depth.

EARTH STRUCTURE AND TECTONIC HYPOTHESES IN THE STUDY AREA

The region under investigation is characterized by strong lateral heterogeneity of the lithospheric structure. One of the main features is the transition from a nearly oceanic structure beneath the Tyrrhenian abyssal plain to a continental-like structure beneath Sicily and Calabria (Morelli *et al.* 1975; Calcagnile & Panza 1981; Calcagnile *et al.* 1982; Scarpa 1982). Many fault systems have been mapped by geological (Frazzetta, Lanzafame & Villari 1982) and geophysical methods (Finetti & Del Ben 1986) (Fig. 1). Although some disagreement still exists among researchers concerning the identification of several faults, at least two large families of fault systems are accepted.

(1) NW–SE to E–W transcurrent faults, characterized by dextral mechanisms in Sicily and the southernmost Tyrrhenian Sea (Trapani to Vulcano faults, Fig. 1), and by sinistral mechanisms to the north (Palinuro and Policastro faults).

(2) Grabens parallel to the Calabrian Arc in Calabria and north-eastern Sicily (ME, MS, CR; Fig. 1). These structures have been the site of several damaging earthquakes in the last few centuries (Mulargia & Boschi 1982; Bottari & Lo Giudice 1987).

An additional feature of this region is the deep earthquakes beneath the Tyrrhenian Sea, along a north-westerly-dipping Wadati–Benioff plane (e.g. Gasparini *et al.* 1982; Anderson & Jackson 1987a).

Several tectonic hypotheses have been proposed in the last few few decades for the study area: active subduction beneath the Southern Tyrrhenian Sea (Barberi *et al.* 1973); rifting dominated by slab sinking and passive subduction (Finetti & Del Ben 1986; Patacca, Sartori & Scandone 1992); growth of mantle diapirs in the whole Tyrrhenian region (Locardi 1988; Locardi & Nicolich 1988); and north-eastward compression due to movement of the African plate (Mantovani *et al.* 1990). In particular, the deep earthquake activity is interpreted as being due to active subduction (Barberi *et al.* 1973; Amato *et al.* 1993), or to passive subduction of a lithospheric slab, which was active before the opening of the Tyrrhenian Sea

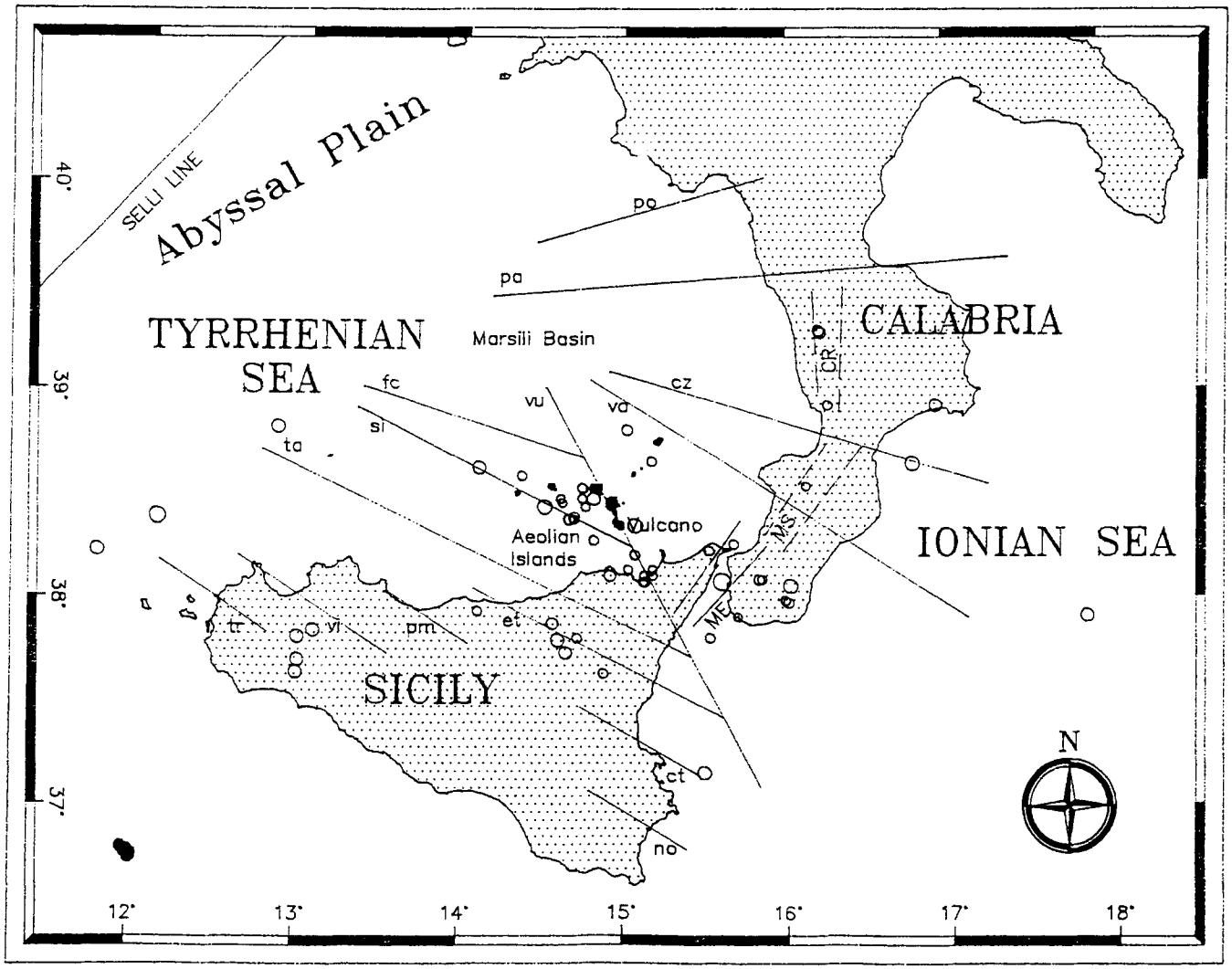

Figure 1. Map of the epicentres of shallow earthquakes with fault-plane solutions. The locations of the main fault systems (tr = Trapani; no = Noto; vi = S. Vito; pm = Palermo; ct = Catania; et = Etna; ta = Taormina; si = Sisifo; fc = Filicudi; vu = Vulcano; va = Capo Vaticano; cz = Catanzaro; pa = Palinuro; po = Policastro; ME = Messina; MS = Mesima; CR = Crati) are from Ghisetti & Vezzani (1982), Finetti & Del Ben (1986).

(Patacca *et al.* 1990), or to asthenolith convective processes (Locardi & Nicolich 1988). The debate about the tectonic modelling of the region is still open. Basic aspects, such as the recent evolution of the interaction between Africa and Europe (still converging?), are a subject of discussion and disagreement among researchers (e.g. Locardi & Nicolich 1988; Mantovani *et al.* 1990; Pollitz 1991; Albarello, Viti & Mantovani 1993; Scandone 1993; Tamburelli *et al.* 1993). New data and investigations are necessary in order to solve the Mediterranean tectonic puzzle. The present estimate of tectonic stress directions in a sector located at the centre of the Mediterranean area is intended to contribute to the understanding of the complex tectonics of the Mediterranean.

METHOD

We used the method of Gephart & Forsyth (1984) and Gephart (1990) for calculating the directions of the stress tensor. Our data base consists of 97 fault-plane solutions (Table 1). Basic assumptions of this method are that (1) stress is uniform in the rock volume investigated, (2) earthquakes are shear dislocations on pre-existing faults, and (3) slip occurs in the direction of the resolved shear stress on the fault plane. The algorithm searches for the stress tensor showing the best agreement with the available fault-plane solutions (FPS). Four stress parameters are calculated: three of them define the orientations of the main stress axes; the other is a measure of relative stress magnitudes:

$$R=(\sigma_2-\sigma_1)/(\sigma_3-\sigma_1),$$

where σ_1, σ_2 and σ_3 are the values of the maximum, intermediate and minimum compressive stresses, respectively. In order to define discrepancies between the stress tensor and observations (FPS), a misfit variable is introduced: for a given stress model, the misfit of a single focal mechanism is defined as the minimum rotation about any arbitrary axis that brings one of the nodal planes, and its slip direction and sense of slip, into an orientation that is consistent with the stress model. Searching through all orientations in space by a grid technique operating in the whole space of stress parameters, the minimum sum of the misfits of all FPS available is found. The confidence limits of the solution are computed by a statistical procedure described in Parker & McNutt (1980) and Gephart & Forsyth (1984). For large data sets, computing time may become a problem and powerful computers may be required, but for the data sets used here, the CPU times on medium-sized machines (such as the IBM 3090) are of the order of a few hours.

The size of the average misfit corresponding to the best stress model provides a guide as to how well the assumption of stress homogeneity is fulfilled (Michael 1987). In the light of results from a series of tests carried out by Wyss *et al.* (1992) and Gillard, Wyss & Okubo (1996) for identifying the relationship between FPS uncertainties and average misfit in the case of uniform stress, we will assume that the condition of homogeneous stress distribution is fulfilled if the misfit, F, is smaller than 6°, and that it is not fulfilled if $F>9°$. In the range $6°<F<9°$, the solution is considered as acceptable, but may reflect some heterogeneity. This criterion for stress homogeneity evaluation in a given data set is, in general, integrated with a detailed analysis of the individual earthquake misfits and computation of the solution confidence limits at several statistical thresholds. A further contribution to the evaluation of the solution significance is given by stability tests carried out on subsamples of the data set.

DATA

Earthquake FPS used as input data for our stress tensor inversion (Table 1) have been taken from the literature, after a critical evaluation of their quality. In total, we selected 97 earthquake FPS, covering the magnitude range 2.5–7.1, the time interval 1908–1991, and depths between the surface and 502 km. As explained in the next section, the only two events available at depths greater than 360 km were excluded from the stress investigation. Epicentres for earthquakes located at depths of less than 50 km in the sector 37–40°N, 11–18°E (Fig. 1) numbered 56. Epicentres of deeper events are shown in Fig. 5.

We used the following criteria for assigning a weight factor to the FPS.

(1) When the polarity distribution on the focal sphere was reported by the authors we used this information for a qualitative evaluation of the level of constraint of the solution: if one of the nodal planes was unconfined to 40°, the solution was excluded (weight $W=0$); if both nodal planes displayed uncertainties of less than 20° we assumed $W=2$; in other cases we assigned $W=1$.

(2) When the polarity distribution was not reported we assigned a weight factor according to the general principle that solutions of older and weaker events should be less reliable: we assigned $W=1$ for events of magnitude 5–6 occurring before 1965; $W=2$ for all events with magnitude greater than 6, and for events of magnitude between 5 and 6 occurring after 1965. $W=0$ was assigned to all other cases.

When more than one solution was available in the literature for the same earthquake, we carefully analysed them. In most of the cases when such a test was possible, we concluded that the weighting criteria described above was able to give us an apparently appropriate choice of the weight value.

An important aspect influencing the FPS quality is the approximate nature of the structural model of the Earth used to locate the earthquakes. This problem is of some concern in the study area because the seismograph network on land is fairly limited, and it is non-existent in areas covered by the sea. For a wider discussion of this topic, see Neri & Wyss (1993), who computed hypocentres and fault-plane solutions of recent earthquakes in the Southern Tyrrhenian region. Neri *et al.* (1996) carried out a series of tests for evaluating the FPS dependence on changes in hypocentral and Earth-structure parameters. Based on our experience with these data, and on considerations reported on the same topic by the authors who computed the FPS used in the present investigation, we conclude that the sample we selected may be considered acceptable for our goal, although significant improvements in this research field in the future can still be expected in the study area as a consequence of network developments and data acquisition on Earth structure.

ANALYSIS

Shallow earthquakes

The inversion of all shallow data for the stress directions yielded a misfit of $F=12.9°$ (set 'shallow' in Table 2), indicating

Table 1. Origin time, magnitude, hypocentral parameters and FPS (taken from the literature) of earthquakes selected for stress inversion. W is the weight assigned to the FPS; its sign indicates reverse (−) or normal (+) mechanism.

Date	O.T. (UTC)	M	Lat(°N)	Lon(°E)	Depth (km)	Strike	Dip	Strike	Dip	W	Bibliography
28/12/08	04.20	7.0	38.12	15.60	10	208	55	349	42	2.0	Gasparini et al.82
13/04/38	02.45	7.1	39.20	15.20	290	30	89	124	16	2.0	Anderson & Jackson 87a
16/03/41	16.35	6.9	38.44	12.12	20	20	53	217	38	2.0	Gasparini et al. 85
11/05/47	06.22	5.6	38.69	16.78	14	302	68	206	77	1.0	Gasparini et al. 82
26/12/52	03.55	6.2	39.96	15.55	264	131	9	199	87	-2.0	Iannaccone et al.,85
23/11/54	13.00	5.3	38.60	15.12	239	297	64	196	69	-1.0	Gasparini et al. 82
01/02/56	15.10	6.2	39.03	15.63	234	188	13	35	78	2.0	Anderson & Jackson 87a
21/05/57	11.44	5.3	38.67	14.11	5	30	74	286	50	1.0	Gasparini et al. 85
23/12/59	09.29	5.3	37.72	14.61	77	77	43	347	87	1.0	"
03/01/60	20.19	6.2	39.26	15.29	283	6	77	179	14	2.0	Gasparini et al. 82
25/03/62	21.38	5.3	39.18	14.58	339	142	89	51	20	1.0	Iannaccone et al. 85
07/09/67	14.09	4.4	37.85	15.94	53	226	85	116	16	1.0	Gasparini et al. 82
31/10/67	21.08	5.0	37.84	14.60	38	89	61	273	80	2.0	"
15/01/68	01.33	5.1	37.89	13.08	20	40	82	302	46	-1.0	"
15/01/68	02.01	5.4	37.75	12.98	10	270	50	156	64	-2.0	Anderson & Jackson 87b
16/01/68	16.42	5.1	37.86	12.98	36	250	58	150	75	-2.0	"
25/01/68	09.56	5.1	37.69	12.97	3	270	64	165	62	-2.0	"
12/02/68	10.18	5.2	37.96	17.87	10	34	72	284	43	-1.0	Gasparini et al. 85
21/04/68	21.09	4.1	39.84	14.91	318	337	69	183	23	1.0	Iannaccone et al. 85
19/05/68	09.37	4.8	38.52	14.82	39	313	45	198	67	-2.0	Gasparini et al. 85
16/06/68	13.03	4.8	37.78	14.65	23	20	80	272	31	-1.0	"
02/04/69	01.38	4.7	39.98	15.24	263	38	24	230	67	-1.0	Iannaccone et al. 85
05/06/70	09.20	4.3	39.18	15.54	267	337	78	192	15	1.0	Gasparini et al. 82
25/04/71	04.39	4.4	39.29	15.29	295	261	45	118	51	1.0	Iannaccone et al. 85
13/04/73	08.12	4.5	38.97	16.92	43	211	89	67	3	1.0	Gasparini et al. 82
20/12/73	17.44	4.9	38.81	14.82	268	256	82	160	34	-2.0	Giardini and Velonà 88
24/01/74	13.19	4.2	39.85	14.58	360	14	79	225	13	1.0	Gasparini et al. 82
22/07/74	07.19	4.5	39.22	15.39	262	342	83	244	40	1.0	Iannaccone et al. 85
23/11/74	18.46	4.7	39.74	18.94	49	275	7	157	87	1.0	Gasparini et al. 82
12/04/75	16.47	4.2	38.45	15.56	178	340	69	68	86	1.0	"
10/08/75	20.55	4.6	38.47	15.64	185	43	52	275	52	1.0	Iannaccone et al. 85
05/11/75	07.46	4.1	38.59	15.93	113	306	63	75	39	1.0	Gasparini et al. 82
18/12/75	13.13	4.0	38.80	15.78	189	347	50	52	63	-1.0	"
17/09/76	01.23	4.4	37.92	14.57	33	322	69	200	36	1.0	"
21/09/76	15.01	4.7	38.80	14.72	299	90	62	180	82	2.0	Giardini and Velonà 88
28/06/77	07.12	5.0	38.60	14.72	260	44	10	146	90	2.0	Iannaccone et al. 85
15/08/77	21.10	4.9	38.79	17.03	74	48	57	157	64	-2.0	Gasparini et al. 82
20/12/77	20.04	4.7	38.44	15.66	169	121	81	292	18	1.0	Iannaccone et al. 85
30/12/77	17.35	5.4	40.00	15.42	283	64	80	304	19	2.0	Anderson & Jackson 87a
30/12/77	18.08	4.7	39.99	15.43	291	306	13	21	89	1.0	Iannaccone et al. 85
11/03/78	19.20	5.6	38.10	16.03	33	183	82	255	31	1.0	Gasparini et al. 82
15/04/78	23.33	5.5	38.39	15.07	21	148	55	254	68	-2.0	Anderson & Jackson 87b
13/08/78	16.53	4.2	38.67	16.01	112	339	22	178	69	1.0	Iannaccone et al. 85
20/01/79	13.49	5.2	38.87	12.86	4	312	68	214	70	-2.0	Gasparini et al. 85
25/03/79	11.36	4.5	39.42	15.19	324	1	43	183	48	1.0	Iannaccone et al. 85
25/07/79	00.18	4.3	39.33	15.09	304	146	64	359	31	-1.0	"
21/09/79	23.47	4.6	39.0	14.83	312	62	50	180	54	2.0	"
08/12/79	04.06	5.4	38.28	11.74	33	254	56	12	55	-2.0	Anderson & Jackson 87b
20/02/80	02.34	4.4	39.32	16.20	10	187	47	62	58	1.0	Gasparini et al. 82
20/02/80	02.40	4.3	39.33	16.19	10	210	48	42	43	1.0	"
28/05/80	19.51	5.7	38.48	14.52	12	52	62	278	37	-2.0	Anderson & Jackson 87b

that this data set is heterogeneous (Wyss *et al.* 1992). Therefore, we selected a number of subsets for inversion, based on spatial extent and magnitude range, in order to reduce misfits below 9°, such that the results can be accepted as based on reasonably homogeneous data.

Magnitude, M, was used as a selection criterion because we noticed that the use of small events, together with large ones, increases the misfits considerably, and because Rebai *et al.* (1992) showed that stress indicators can follow perturbations of the regional stress field of dimensions equal to, or somewhat

Table 1. (*Continued.*)

13/10/80	03.44	4.6	39.91	12.98	502	117	28	7	80	1.0	Iannaccone et al. 85
24/11/80	02.39	4.3	39.05	14.56	319	184	64	12	27	1.0	"
01/01/81	23.09	4.3	39.93	13.54	442	2	50	236	55	-1.0	"
10/05/81	02.44	4.5	39.53	15.31	291	45	59	313	85	-1.0	"
30/03/82	02.16	4.9	38.47	15.38	211	126	40	335	54	-1.0	"
21/06/82	04.18	4.3	38.68	14.92	294	188	53	11	38	1.0	"
21/03/84	01.12	5.1	39.42	15.23	281	137	21	227	90	2.0	Anderson & Jackson 87b
06/04/88	01.25	3.1	38.57	14.75	8	238	76	148	89	1.0	Neri and Wyss 92
11/04/88	01.50	2.6	38.12	15.12	12	46	58	174	45	2.0	"
28/05/88	05.57	3.2	38.32	14.82	20	71	72	263	18	2.0	"
30/05/88	10.06	3.6	38.43	14.70	12	97	46	310	48	1.0	"
05/06/88	12.43	3.7	38.42	14.67	12	68	35	319	77	2.0	"
10/06/88	01.31	2.6	38.18	15.18	11	124	74	244	29	1.0	"
21/07/88	17.18	2.8	37.95	15.70	33	296	88	204	21	1.0	"
23/07/88	17.58	3.6	38.72	15.63	85	207	86	354	4	-2.0	"
07/10/88	16.22	2.6	38.50	14.63	11	209	22	301	88	-1.0	"
07/11/88	14.26	3.6	38.13	15.83	15	59	4	198	86	-1.0	"
23/01/89	08.22	3.0	37.85	15.53	18	189	87	85	8	1.0	"
25/04/89	01.08	3.3	37.98	14.10	10	82	67	337	58	1.0	"
02/05/89	11.48	99.	38.52	14.75	8	187	28	294	80	1.0	"
26/05/89	22.19	3.1	38.15	15.13	12	68	81	330	46	-2.0	"
21/06/89	16.46	2.8	38.18	15.03	12	120	76	316	14	-2.0	"
24/06/89	02.34	3.3	37.85	14.72	13	77	31	224	62	1.0	"
18/07/89	05.08	2.9	38.48	14.77	11	132	55	303	34	-2.0	"
25/07/89	01.47	3.0	38.53	15.57	239	165	46	262	81	1.0	"
29/08/89	22.46	3.0	38.30	15.67	9	198	88	289	52	-1.0	"
12/09/89	01.32	2.6	38.42	14.70	12	101	47	248	47	-1.0	"
26/09/89	16.38	2.8	38.52	14.62	14	133	87	247	6	1.0	"
08/02/90	17.50	3.1	38.97	16.25	9	36	85	302	47	-1.0	"
18/02/90	00.28	3.3	38.12	15.13	23	166	77	44	2	2.0	"
26/02/90	03.11	3.3	38.63	14.38	20	69	43	286	53	2.0	"
28/03/90	05.47	4.2	38.15	14.92	24	207	55	320	60	2.0	"
04/04/90	15.03	3.2	38.25	15.07	15	113	79	281	10	1.0	"
10/05/90	06.47	3.0	38.27	15.52	21	11	72	207	17	-2.0	"
15/09/90	03.11	3.3	38.13	15.85	17	157	39	6	54	1.0	"
22/09/90	10.05	3.3	38.70	15.17	9	177	87	279	10	1.0	"
11/11/90	09.11	3.8	38.43	15.40	100	101	56	203	72	1.0	"
13/12/90	00.24	5.4	37.20	15.50	10	8	90	270	60	-2.0	Giardini et al. 92
18/12/90	04.38	2.5	38.15	15.18	10	71	81	310	15	-1.0	Neri and Wyss 92
27/04/90	00.57	3.3	38.78	15.67	62	109	19	246	75	-1.0	"
21/08/90	02.42	3.7	39.05	15.95	52	37	45	232	45	1.0	"
24/09/91	00.04	3.1	37.68	14.88	28	183	65	313	34	1.0	"
25/09/91	13.21	3.4	38.03	16.00	16	2	87	125	4	2.0	"
25/09/91	14.53	3.7	38.02	16.02	17	151	89	61	89	-1.0	"
03/10/91	02.40	3.8	38.85	15.02	12	75	82	326	22	-1.0	"
22/10/91	00.35	99.	38.58	16.12	9	44	82	265	9	1.0	"

larger than, the dimensions of the stress indicator. We propose that FPS of earthquakes with $M=3$ and $M>5$ gauge the stress directions in volumes of a few kilometres and up to 100 km, respectively. Therefore, we expect the following effects from combining data for small and large earthquakes:

(1) For volumes with uniform stress throughout, the combined data set will yield a well-constrained result with a small misfit.

(2) For volumes which contain localized perturbations of the stress field, two situations may arise. (a) If the small earthquakes are randomly distributed in the volume they may sense random perturbations. In this case an increase of F, and a widening of the confidence limits, are expected. The small events cannot define the stress in any subvolume in this case. (b) If the small earthquakes are confined to one small subvolume, they may define a locally different stress field. This will also increase F in the total combined data set, but the local stress directions can be estimated for the subvolume containing the small earthquakes.

Selecting earthquakes with $M \geq 5$ for inversion leads to a significant reduction of the misfit to 8.6° (set M5, Table 2, Fig. 2). By excluding four additional earthquakes from this set, the northernmost event and three events near Messina (Fig. 2), the misfit was dramatically reduced to $F=3.1°$ (set M5modified, Table 2). The stress directions, especially σ_1, are well defined (Fig. 6a), in spite of the small number of events

Table 2. Stress inversion results for the earthquake sets analysed in the present study. N and F are, respectively, the number of events and the 'average misfit' corresponding to the stress solution.

SET	Depth	N	F	σ_1		σ_2		σ_3		R	Definition
				Dip	Strike	Dip	Strike	Dip	Strike		
Shallow	0-50	56	12°.9	56	185	31	348	12	86	0.5	Fig. 1
M5	0-50	16	8.6	28	181	46	57	31	289	0.4	Fig. 2
M5modif	0-50	12	3°.1	29	175	35	288	41	56	0.9	Fig. 2
Messina M4	0-50	9	2°.8	56	167	9	63	32	327	0.6	Fig. 3
Messina M25	0-50	20	4°.6	73	143	8	26	15	293	0.6	Fig. 3
WSicily	0-50	17	7°.4	34	296	32	51	39	172	0.3	Fig. 4
DeepM45	125-510	22	7°.6	70	357	12	231	16	138	0.7	
Deeper230	230-360	20	5°.9	74	353	9	230	13	138	0.9	Fig. 5

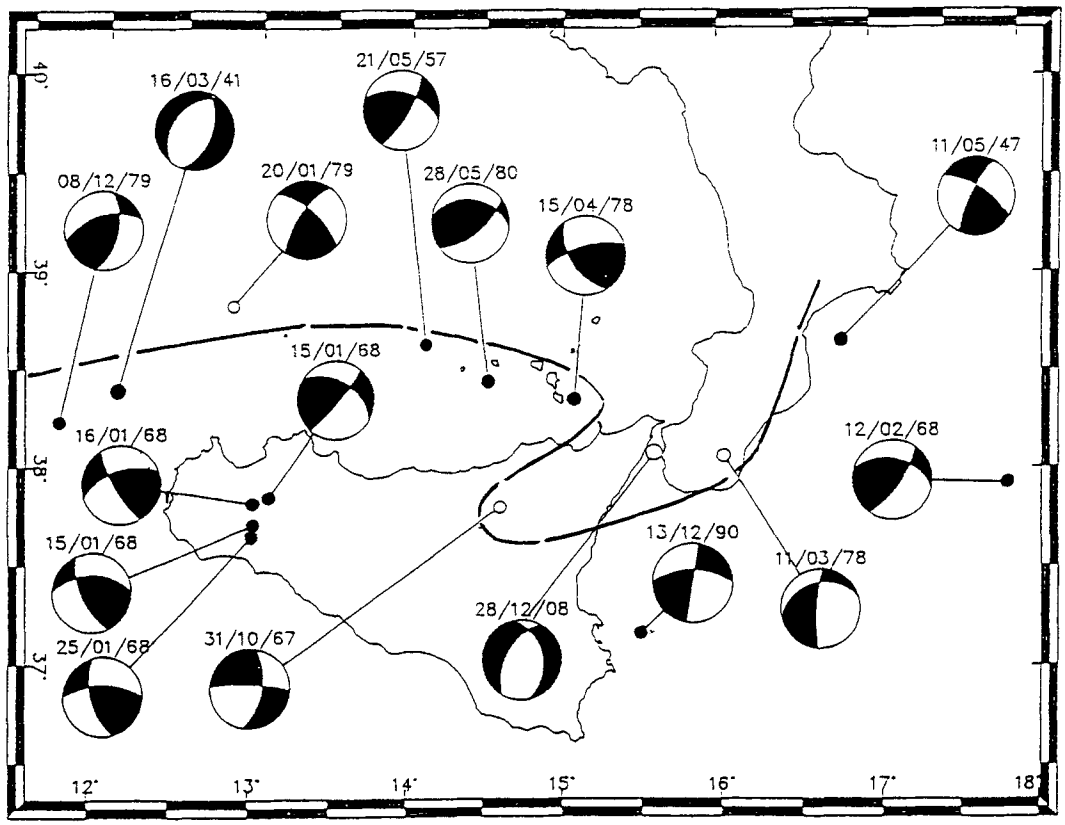

Figure 2. Epicentre map with fault-plane solutions for earthquakes of magnitude $M \geq 5.0$ located at depths of less than 50 km (set 'M5'). Solid dots mark events used in set 'M5modified'. The curved line separates different stress domains (see text for details).

used ($N = 12$). We conclude that the larger shallow earthquakes reliably define the regional stress directions in the area outlined by the epicentres, marked by solid dots in Fig. 2.

Separating the data of all magnitudes into an eastern and a western set leads to reductions of the average misfits to $F = 9°$ and $F = 11°$, respectively; these values are still large. By examination we found that the earthquakes with the worst misfits in both sets were located at the margins of the respective volumes. Therefore, we excluded some of the events along the margins from the inversion procedure, and received acceptable misfits. The 'Messina' data set was obtained from the eastern group of events by eliminating those shown as open circles in Fig. 3. This set of 20 earthquakes with $M > 2.5$ yielded a misfit of $F = 4.6°$, and a value of $F = 2.8°$ if only $M \geq 4$ events were used (Table 2). The Messina data set defines an extensional stress regime in north-eastern Sicily and south-western Calabria (Figs 6b–c). The 'WSicily' data set (solid dots in Fig. 4) were inverted separately from the data in the Tyrrhenian sea, because the latter (open circles in Fig. 4) showed generally large misfits in the joint inversion (western set). However, the WSicily confidence areas are not yet satisfactory and the misfit $F = 7.4°$ suggests that some heterogeneity remains in this data set

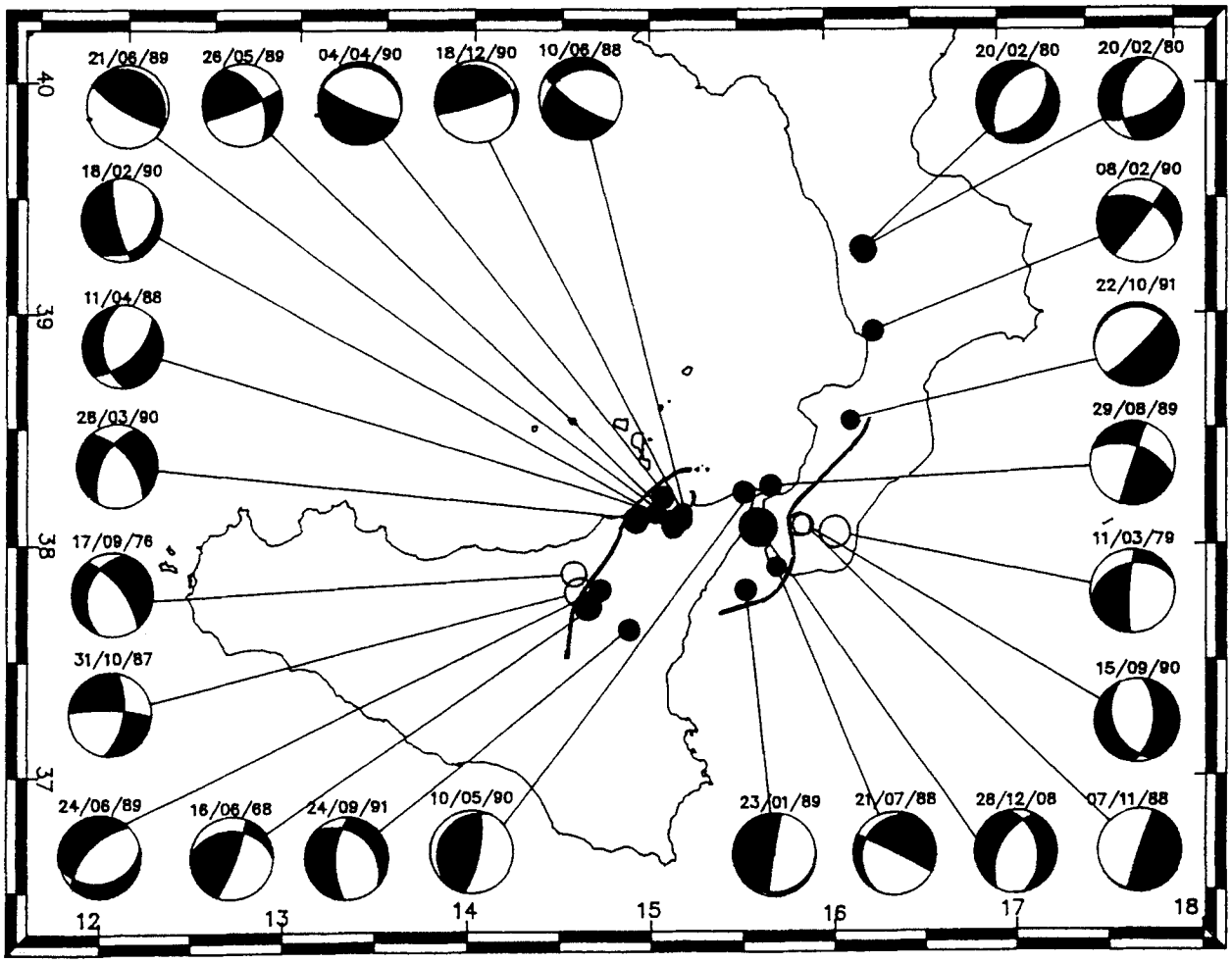

Figure 3. Epicentre map and fault-plane solutions for earthquakes of magnitude $M \geq 2.5$ located at depths of less than 50 km in north-eastern Sicily and southern Calabria (solid dots mark events used in data set 'Messina'). The radii of the epicentre circles are proportional to earthquake size (magnitude range 2.5–7.0). The curved lines separate different stress domains (see text for details).

(Fig. 6d). This finding confirms the preliminary information from Neri & Wyss (1993) on local stress heterogeneities in northern Sicily and the Aeolian Islands area.

Deep earthquakes

Focal mechanisms for 41 earthquakes with hypocentres deeper than 50 km, located in the Tyrrhenian area, were found in the literature (Table 1). We excluded several of these in the depth range of 50 to 100 km from analysis because they were scattered throughout the study area, and not associated with the Wadati–Benioff zone. The two earthquakes with a depth greater than 360 km (depths of 442 and 502 km) were also excluded, because they were far separated from the bulk of the deep events, which had focal depths between 230 and 360 km.

Two deep data sets yielded acceptable results in terms of the requirement for $F < 9°$. The set 'DeepM45', including all earthquakes with focal depth $h > 125$ km and $M \geq 4.5$, resulted in $F = 7.6°$ (Fig. 6f and Table 2), and the data set 'Deeper230', made up of events between 230 and 360 km depth within the Wadati–Benioff zone (Fig. 5), yielded $F = 5.9°$ (Fig. 6e and Table 2). The reasons for inverting the data set from below 230 km depth separately were that a change in dip of the Wadati–Benioff zone may exist at this depth (Anderson & Jackson 1987a), and that the individual misfits above this depth tended to be high.

DISCUSSION

The reduction of the average misfit from 12.9° for the whole data set of shallow earthquakes to values in the range $2.8° \leq F \leq 7.4°$ in subsets (Table 2) suggests that the stress directions are heterogeneous in the area studied, but that they are uniform in subvolumes. The great stability of the stress directions in subsets of the data gives confidence in the reliability of the solutions obtained. For all of the subsets for which solutions are presented in Table 2 we found the same best solutions, within 10° to 20°, regardless of adding or subtracting a few events located along the margins of the data set. To arrive at a final choice of events for a subset our procedure was as follows. We selected all events located in an area of similar tectonic style, as expressed by the geological data (e.g. NE Sicily–Calabria). In all these choices the resulting inversions showed smaller average misfits than that of the entire data set, and the earthquakes with the largest individual misfits were located at the margins of the areas considered.

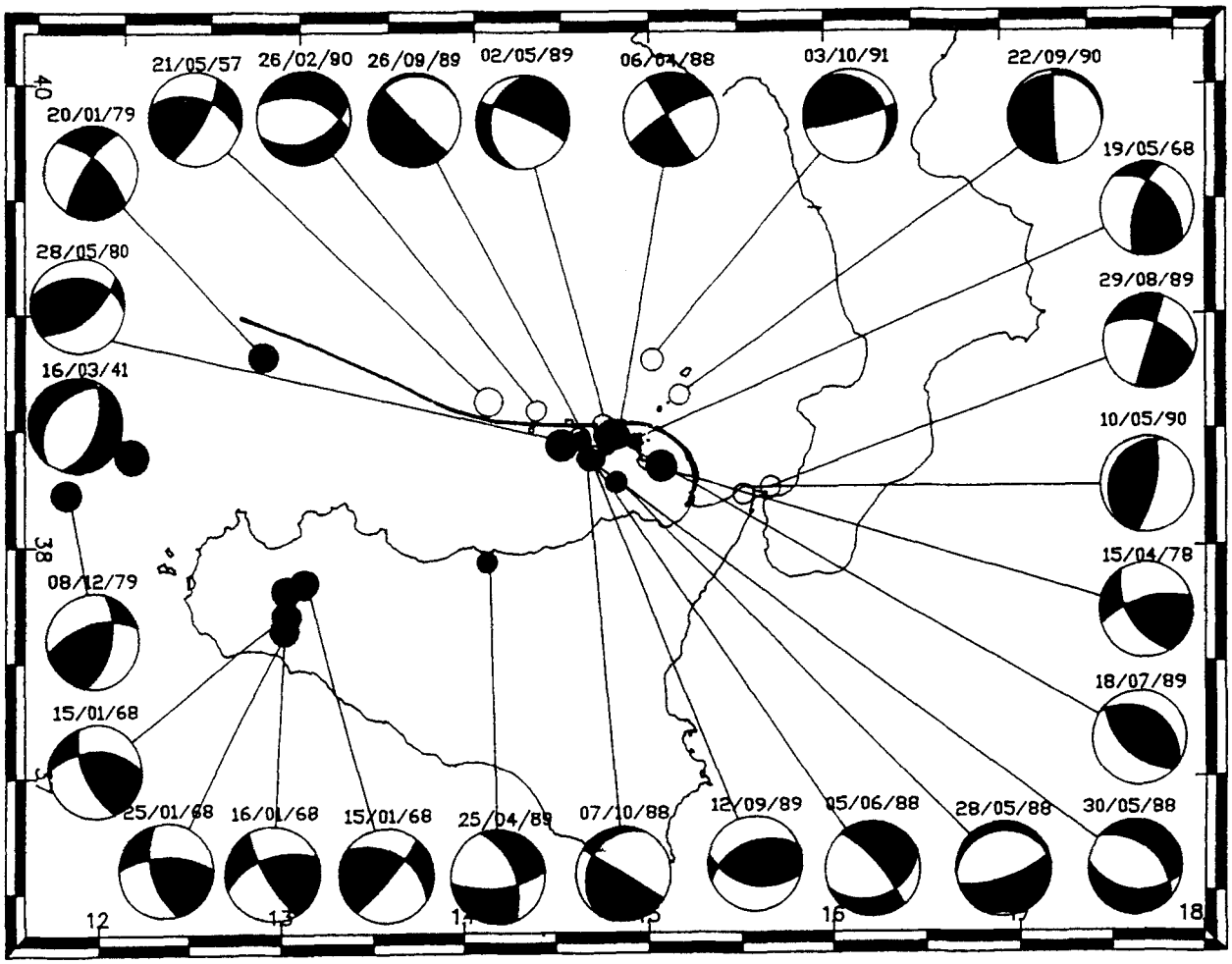

Figure 4. Epicentre map and fault-plane solutions for earthquakes of magnitude $M \geq 2.5$ located at depths of less than 50 km in northern Sicily and the Tyrrhenian sea. Solid dots mark events used in the dataset 'WSicily'. The radii of the epicentre circles are proportional to the earthquake sizes (magnitude range 2.5–6.9). The curved line separates different stress domains (see text for details).

We then redefined the boundaries of the selected areas such that events with misfits larger than 15° were excluded as much as possible. Data from earthquakes surrounded by other events with small misfits were never excluded. Our assumption is that events with large misfits, located along the margins, originate in a stress field different from that of the analysed set. After excluding these events from the inversion of the data set in question we added them to the other adjacent earthquakes, and if there were enough events available in this additional area we inverted for this data set. If eight or fewer events are located in such an area we cannot attempt inversions, and the events remain excluded from the analysis.

The Messina data set clearly defined itself in the way described above. The events located to the east, which have been only partly reported in Fig. 3 for space reasons (open circles), were immediately noticeable due to their large misfits. Their fault-plane solutions were not compatible with the stress tensor of normal faulting, which was required by the rest of the events in the Messina data set (Figs 6b–c, 7b–c and Table 2). The Messina data set shows a satisfactory misfit of $F = 4.6°$ if all events with $M > 2.5$ are used, and F drops to 2.8° for $M >= 4.0$ events (Table 2). The stress directions estimated from the two data sets are the same, within about 15°, and those computed from the largest data set (Messina-M25) are very well constrained at the 90 per cent confidence level (Fig. 6b). Normal faulting with a WNW extension direction found from inversion of the Messina set conforms to orientation of the stress tensor required to open the grabens mapped geologically in Messina and southern Calabria by pure normal faulting. We conclude that the normal stress field, as shown in Figs 6(b) and (c), is representative of the entire area in north-eastern Sicily and southern Calabria outlined by the solid epicentres in Fig. 3. We consider this result as meaningful, because we have used up to 20 earthquakes to define the solutions, the stress orientations are stable when varying the sample, the constraints are reasonable (Figs 6b and c), and the misfits are small (4.6° and 2.8°). We propose that the curved line crossing southern Calabria in Fig. 3, which separates the eastern epicentres with large misfits from the epicentres in the Messina set, represents a change from normal faulting (to the NW) to a different stress field. The eastern earthquakes are not numerous enough to define an inversion result by themselves, but they fit the stress field found by inversion of the larger events in the rest of the study area surrounding the Messina data set, as discussed below.

The inversion of data from $M \geq 5$ earthquakes yielded a remarkably small misfit of 3.1° (M5modified in Table 2) when the three events belonging to the Messina set and the northern-

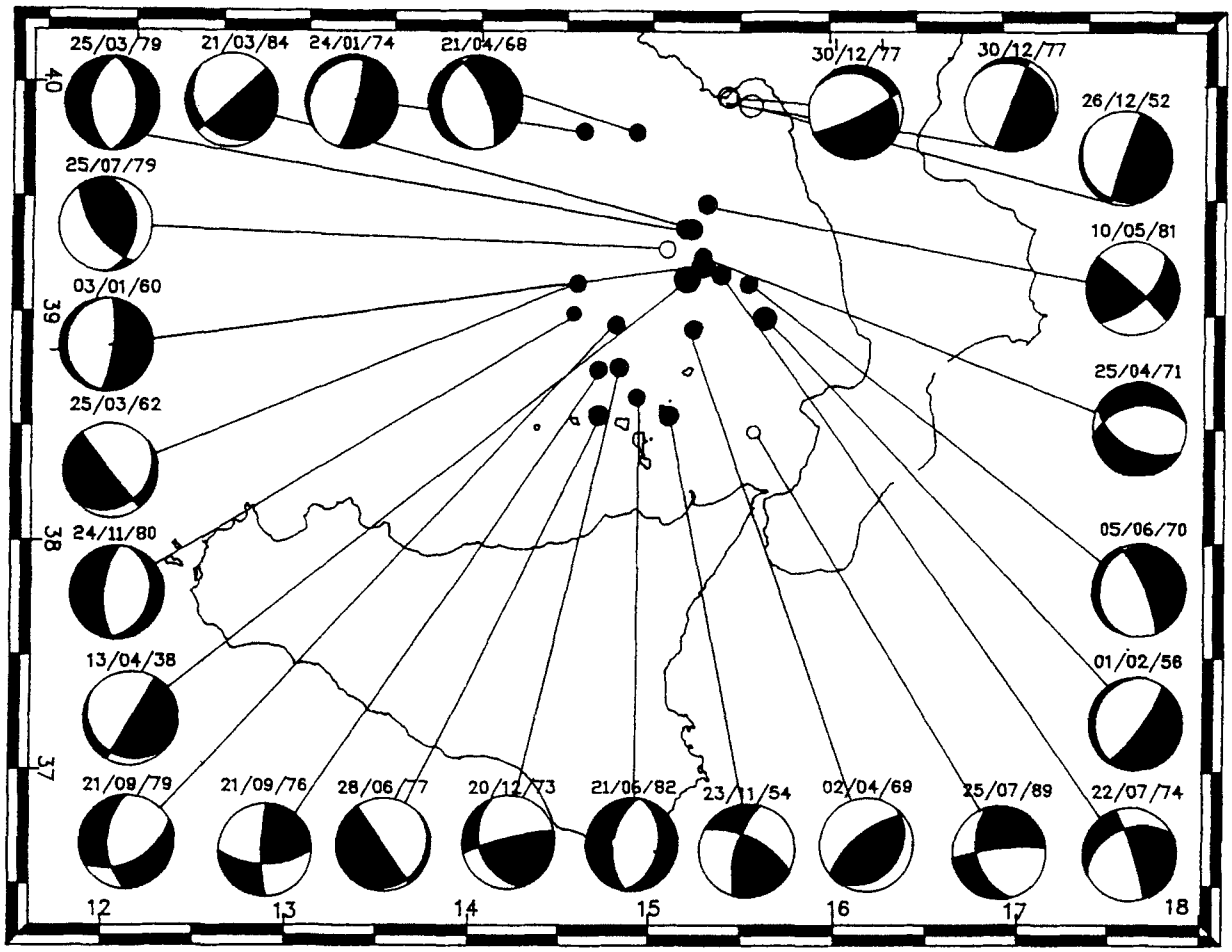

Figure 5. Epicentre map and fault-plane solutions for earthquakes of magnitude $M \geq 3.0$ with hypocentral depths 230 to 360 km below the Tyrrhenian sea. Solid symbols mark events used in the dataset 'Deeper230'; open symbols mark events located outside the major trend of deep-earthquake activity. The radii of the epicentre circles are proportional to earthquake size (magnitude range 3.0–7.1).

most event in the entire data set were excluded (Figs 2 and 7a). Without excluding these events, the *M*5 data set yields $F = 8.6°$, and thus approaches the 'unsatisfactory' category, as defined by Wyss *et al.* (1992). The σ_1 direction estimated by the M5modified set is very well constrained (Fig. 6a), in spite of the small number of fault-plane solutions available ($N = 12$). We accept this result as meaningful and interpret it as showing that a regional stress field is present in the southern Tyrrhenian sea, northern Sicily and along the SE coast of Calabria (outlined by the solid epicentres in Fig. 2; see also Fig. 7a) with a north–south σ_1 direction. This stress field is defined by earthquakes of rupture length of the order of 10 km in a volume with dimensions exceeding 100 km. Our finding is compatible both with the aforementioned large-scale stress pattern proposed by Rebai *et al.* (1992) and with the orientations of earthquake *P*-axes found by Udias & Buforn (1991) to the west and to the east of Sicily along the Mediterranean belt.

Within the whole region, perturbations of the stress field exist on a scale of tens of kilometres, as evidenced by the increase of the average misfit if smaller earthquakes are included in the inversion. The *M*3 earthquakes have dimensions of the order of 1 km, and are therefore subject to locally perturbed stress fields. This situation is similar to that described for southern France by Rebai *et al.* (1992) in their first three figures. An exception is the Messina data set, where the perturbation of the stress directions covers an area large enough to influence large ruptures as well as small ones (Fig. 3).

A schematic synthesis of our results is presented in Fig. 8, where the regional stress field is sketched by double arrows (1) along the margins of the map. The extensional stress field causing normal faulting in north-eastern Sicily and south-western Calabria is represented by extensional double arrows (2) and a graben structure in the Messina straits. We propose that within a regional setting of north–south compression, most likely due to the collision between Africa and Europe, there is a well-defined perturbation in the area of the Messina data set (Figs 3, 7 and 8). In the Tyrrhenian sea and north-western Sicily the stress directions also differ locally from the regional stress defined by the data set M5modif. We first inverted the data set for the western part of the study area (solid plus open symbols in Fig. 4), which yielded an unacceptably large average misfit of $F = 11°$. Most of the large individual misfits were associated with northern epicentres. By the exclusion of data from the northern Aeolian Islands and the Messina area (open symbols in Fig. 4), the average misfit was reduced to $F = 7.4°$ using the 17 south-western events. Further reductions of F could not be achieved by additional

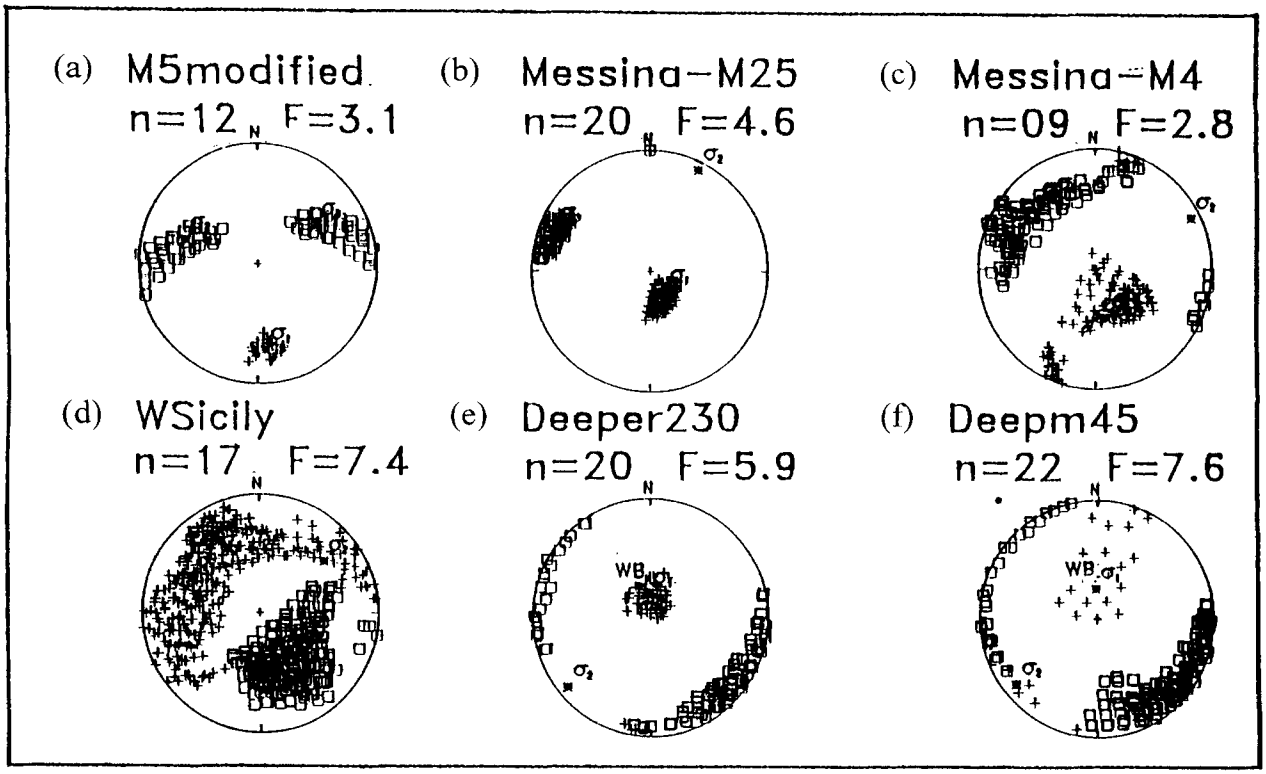

Figure 6. Lower-hemisphere projections of the directions of the principal stresses for the datasets indicated in the headings. Crosses and squares define the 90 per cent confidence limits of the greatest and least principal-stress orientations, respectively. The number, N, of events used and the misfit, F, are shown for each solution. The projection of the Wadati–Benioff zone (WB) is indicated for comparison with stress directions estimated for deep earthquakes. The numerical values relating to all stress solutions reported in this figure are given in Table 2. The sectors concerned with the respective data sets are indicated in Fig. 7.

geographical limitations of the data set. The resulting average misfit of $F = 7.4°$ and the confidence areas of the solution are not fully satisfactory for the WSicily data (Fig. 6d). Both measures of the quality of the result are inferior to the results of the other final data sets presented in Fig. 6 and Table 2. Therefore, we accept this as a preliminary result and plot it using dashed arrows (3) in Fig. 8 until more data become available to define the stress directions separately for different parts of western Sicily and the southern Tyrrhenian. The data from the northern Aeolian Islands, which we did not use in this inversion (the northermost open circles in Fig. 4), are not numerous enough for inversion by themselves. An estimate of the stress direction for this area must wait until additional fault-plane solutions become available.

The stress directions estimated from deep earthquakes in the Wadati–Benioff zone are also judged as reliable: they are stable (the same within less than 10°), regardless of whether all events deeper than 50 km or some subsets (Table 2) are used; and the misfit (5.9°) and the confidence areas (Fig. 6e) are acceptably small for dataset Deeper230. Other authors have pointed out that the P-axes point, on average, down-dip in the Tyrrhenian Wadati–Benioff zone (e.g. Gasparini *et al.* 1982; Anderson & Jackson 1987a). Here we show more rigorously that σ_1 is directed subparallel to the plunge of the deep seismic zone, and that σ_2 is aligned approximately along its strike (Figs 6e–f). The σ_1 orientation within the deep seismic zone is also shown schematically in Fig. 8 (arrows 4). It has been suggested that down-dip compression over a whole slab is related to decoupling of the subducting plate from its overriding plate (Hasegawa 1989). We note that, if the assumptions of Kanamori (1977) concerning slab retreat are realistic, the decoupling model is supported in the Tyrrhenian by the observed continuity of the Benioff zone and its change to a shallower dip below about 250 km (Anderson & Jackson 1987a). Finally, possible evidence that subduction is no longer occurring in the area is provided by the lack of large shallow thrusting events at the surface projection of the Benioff zone (Anderson & Jackson 1987a,b). All the above information and stress-tensor results appear to be in agreement with tectonic models assuming passive subduction in the region (e.g. Patacca *et al.* 1992).

In summary, in the lithosphere of Sicily and the surrounding areas, we have found that regional north–south compression is active (Fig. 8). Within this stress field, defined by the larger earthquakes, local differences in the stress directions exist. In the lithosphere of the central Tyrrhenian we do not have enough data to define the local direction. In western Sicily a local direction of compression to the NW is poorly defined by the available data. Near Messina, active extension in a WNW direction is well defined and has resulted in the opening of graben structures. The fault-plane solutions in the deep seismic zone show that the deep slab acts as a stress guide, and is in down-dip compression. With more fault-plane solutions, more details of the local stress field may be resolved in the future.

ACKNOWLEDGMENTS

The efforts of M. Wyss were in part supported by the Wadati endowment at the Geophysical Institute of the University of

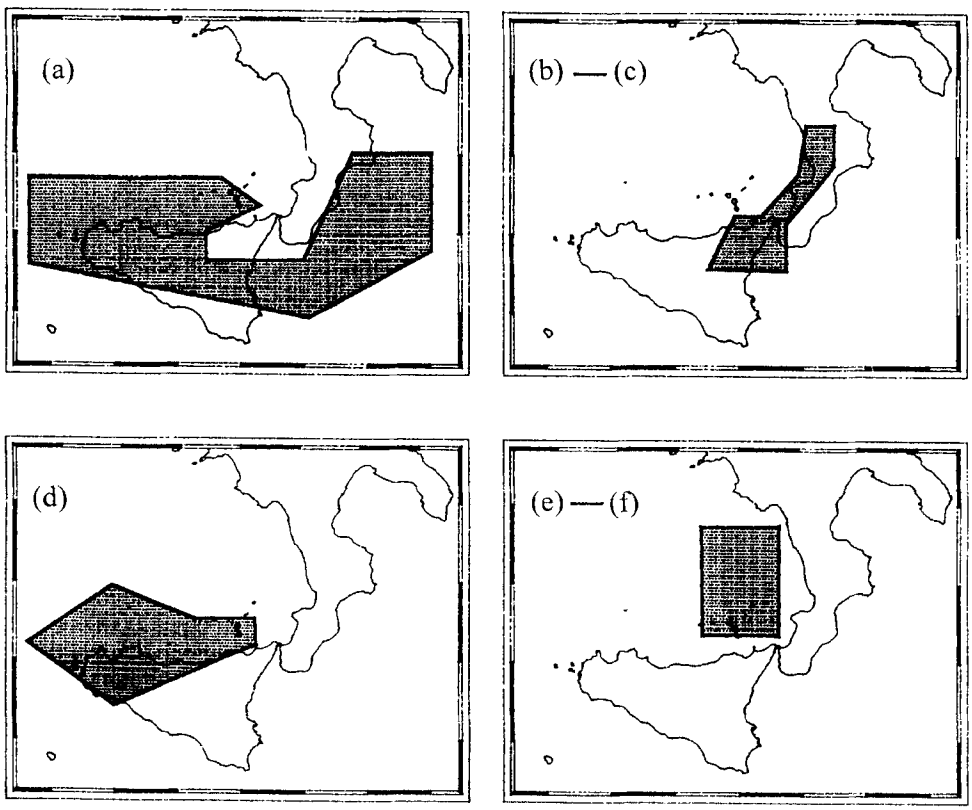

Figure 7. Schematic representation of sectors related to data sets M5modified (a), Messina-M25 and Messina-M4 (b–c), WSicily (d), Deeper230 and DeepM45 (e–f) (results from stress inversion of these data sets are given in Fig. 6 and Table 2).

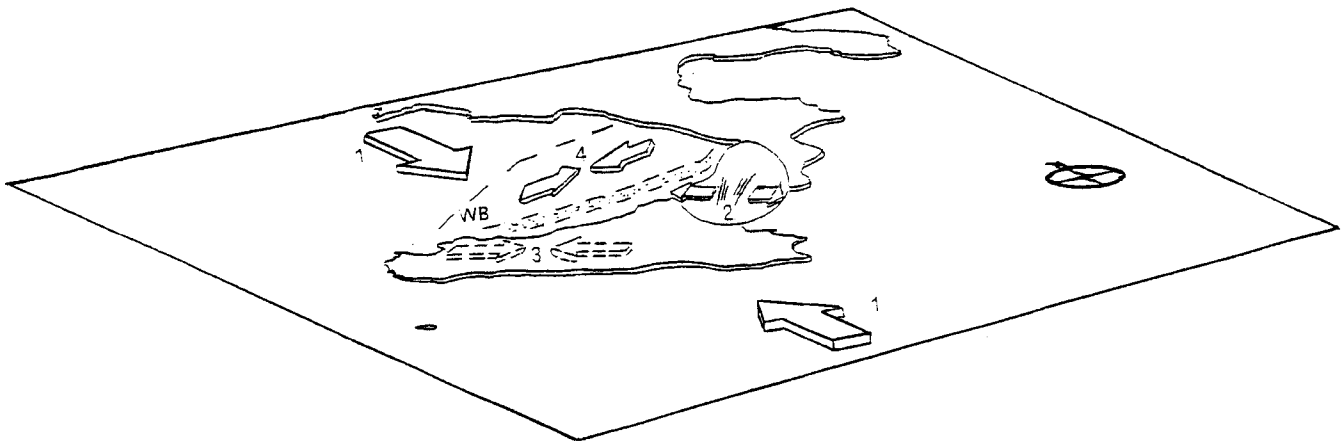

Figure 8. Schematic representation of the stress directions estimated from the four data sets with useful results (1: M5modif, overall stress field estimated from the larger earthquakes; 2: Messina-M25, local graben dynamics; 3: WSicily, the dashed double arrows symbolize the fairly low quality of the results; 4: Deeper230, down-dip compression in the Wadati–Benioff zone, WB).

Alaska, Fairbanks. The work also received financial contributions from CNR (Progetti Bilaterali, N. 93.02151.CT05) and MPI-40% (1993, G. Neri).

REFERENCES

Albarello, D., Viti, M. & Mantovani, E., 1993. Modellazione numerica del quadro deformativo recente della Sicilia e zone circostanti, 12th GNGTS-CNR Meeting, Rome, Abs. Vol., p. 58.

Amato, A., Alessandrini, B., Cimini, G., Frepoli, A. & Selvaggi, G., 1993. Active and remnant subducted slabs beneath Italy: evidence from seismic tomography and seismicity, *Ann. Geophys.*, **36,** 201–214.

Anderson, H. & Jackson, J., 1987a. The deep seismicity of the Tyrrhenian Sea, *Geophys. J. R. astr. Soc.*, **91,** 613–637.

Anderson, H. & Jackson, J., 1987b. Active tectonics of the Adriatic region, *Geophys. J. R. astr. Soc.*, **91,** 937–983.

Barberi, F., Gasparini, P., Innocenti, F. & Villari, L., 1973. Volcanism of the Southern Tyrrhenian Sea and its geodynamic implications, *J. Geophys. Res.*, **78,** 5221–5232.

Bottari, A. & Lo Giudice, E., 1987. Structural studies on the strait of Messina. The seismotectonic data, *Doc. et Trav. IGAL*, Paris, **11,** 115–125.

Calcagnile, G. & Panza, G.F., 1981. The main characteristics of the lithosphere–asthenosphere system in Italy and surrounding regions, *Pageoph,* **119,** 865–879.

Calcagnile, G., D'Ingeo, F., Farrugia, P. & Panza, G.F., 1982. The lithosphere in the central Eastern Mediterranean area, *Pageoph,* **120,** 389–406.

Cristofolini, R., Ghisetti, F., Scarpa, R. & Vezzani, L., 1985. Character of the stress field in the Calabrian Arc and Southern Apennines (Italy) as deduced by geological, seismological and volcanological information, *Tectonophysics,* **117,** 39–58.

Finetti, I. & Del Ben, A., 1986. Geophysical study of the Tyrrhenian opening, *Boll. Geof. Teor. Appl.,* **28,** 755–155.

Frazzetta, G., Lanzafame, G. & Villari, G., 1982. Deformazioni e tettonica attiva a Lipari e Vulcano (Eolie), *Mem. Soc. Geol. It.,* **24,** 293–297.

Gasparini, C., Iannaccone, G., Scandone, P. & Scarpa, R., 1982. Seismotectonics of the Calabrian arc, *Tectonophysics,* **84,** 267–286.

Gasparini, C., Iannaccone, G. & Scarpa, R., 1985. Fault-plane solutions and seismicity of the Italian peninsula, *Tectonophysics,* **117,** 59–78.

Gephart, J.W., 1990. Stress and the direction of slip on fault planes, *Tectonics,* **9,** 845–858.

Gephart, J.W. & Forsyth, W.D., 1984. An improved method for determining the regional stress tensor using earthquake focal mechanism data: applications to the San Fernando earthquake sequence, *J. geophys. Res.,* **89,** 9305–9320.

Ghisetti, F., 1984. Recent deformations and the seismogenic source in the Messina Strait (Southern Italy), *Tectonophysics,* **109,** 191–208.

Ghisetti, F. & Vezzani, L., 1982. Different styles of deformation in the Calabrian Arc (southern Italy): implications for a seismotectonic zoning, *Tectonophysics,* **85,** 149–165.

Giardini, D. & Velonà, M., 1988. Una tecnica di correlazione applicata allo studio del campo di sforzo nel Basso Tirreno, *Proc. 7th GNGTS-CNR Mtg,* Rome, 471–480.

Giardini, D., Boschi, E. & Palombo, B., 1992. Moment tensor inversion from Mednet data regional earthquakes of the Mediterranean, *Geophys. Res. Lett.,* **20,** 273–276.

Gillard, D., Wyss, M. & Okubo, P., 1996. Stress and strain tensor orientations in the south flank of Kilauea, Hawaii, estimated from fault plane solutions, *J. geophys. Res.,* **101,** in press.

Hasegawa, A., 1989. Seismicity: subduction zone, in *The Encyclopedia of Solid Earth Geophysics,* pp. 1054–1061, ed. James, D.E., Van Nostrand Reinhold Company, New York, NY.

Iannaccone, G., Scarcella, G. & Scarpa, R., 1985. Terremoti intermedi e profondi del Marc Tirreno. Rilocalizzazioni con il metodo JHD e meccanismi focali, *Proc. 4th GNGTS-CNR Mtg,* Rome, 145–157.

Kanamori, H., 1977. Seismic and aseismic slip along subduction zones and their tectonic implications, in *Island Arcs, Deep Sea Trenches and Back-arc Basins,* pp. 163–174, eds Talwani, M. & Pitman, W.C., AGU, Washington, DC.

Locardi, E., 1988. The origin of the Apenninic arcs, *Tectonophysics,* **146,** 105–123.

Locardi, E. & Nicolich, R., 1988. Geodinamica del Tirreno e dell'Appenino centro meridionale: la nuova carta della Moho, *Mem. Soc. Geol. It.,* **6,** 121–140.

Mantovani E., Babbucci, D., Albarello, D. & Mucciarelli, M., 1990. Deformation pattern in the Central Mediterranean and behaviour of the African/Adriatic promontory, *Tectonophysics,* **179,** 63–79.

McKenzie, D.P., 1969. The relation between fault plane solutions for earthquakes and the directions of the principal stresses, *Bull. seism. Soc. Am.,* **59,** 591–601.

Michael, A.J., 1987. Use of focal mechanisms to determine stress: a control study, *J. geophys. Res.,* **92,** 357–368.

Morelli, C., Giese, P., Cassinis, R., Colombi, B., Guerra, I., Luongo, G., Scarascia, S. & Schutte, K.G., 1975. Crustal structure of Southern Italy. A seismic refraction profile between Puglia–Calabria–Sicily, *Boll. Geofis. Teor. Appl.,* **17,** 182–210.

Mulargia, F. & Boschi, E., 1982. The 1908 Messina earthquake and related seismicity, *Proc. E. Fermi Summer School Geophys,* Varenna, pp. 493–518, Springer-Verlag.

Neri, G. & Wyss, W., 1992. Inversione del tensore deglisforzi delle soluzioni a faglia piana dei terremoti del Tirreno Meridionale, *Proc. 11th GNGTS-CNR Mtg,* Rome, 159–162.

Neri, G. & Wyss, M., 1993. Preliminary results from stress tensor inversion of earthquake fault plane solutions in the Southern Tyrrhenian region, *Boll. Geof. Teor. Appl.,* **XXXV,** 349–362.

Neri, G., Caccamo, D., Cocina, O. & Montalto, A., 1996. Geodynamic implications of recent earthquake data in the Southern Tyrrhenian Sea, *Tectonophysics,* in press.

Parker, R.L. & McNutt, M.K., 1980. Statistics for the one-norm misfit measure, *J. geophys. Res.,* **85,** 4429–4430.

Patacca E., Sartori, R. & Scandone, P., 1992. Tyrrhenian basin and Appeninic arcs: kinematic relations since Late Tortonian times. *Mem. Soc. Geol. It.,* **45,** 425–451.

Pollitz, F.F., 1991. Two stage model of African absolute motion during the last 30 million years, *Tectonophysics,* **194,** 91–106.

Rebai, S., Philip H. & Taboada, A., 1992. Modern tectonic stress field in the Mediterranean region: evidence for variation in stress directions at different scales, *Geophys. J. Int.,* **110,** 106–140.

Scandone, P. & Patacca, E., 1984. Tectonic evolution of the Central Mediterranean area, *Ann. Geophys.,* **2,** 139–142.

Scandone, P., 1993. Modello sismotettonico d'Italia, *12th GNGTS-CNR* Mtng, Rome, Abs. Vol., p. 26.

Scarpa, R., 1982. Travel-time residuals and three-dimensional velocity structure of Italy, *Pageoph,* **120,** 583–606.

Tamburelli, C., Mantovani, E., Albarello, D. & Babbucci, D., 1993. Quadro cinematico nell'area mediterranea centro-orientale, *12th GNGTS-CNR Mtng,* Rome, Abs. Vol., p. 55.

Udias, A. & Buforn, E., 1991. Regional stresses along the Eurasia–Africa plate boundary derived from focal mechanisms of large earthquakes, *Pageoph,* **136,** 433–448.

Wyss, M., Liang, B., Tanigawa, W.R. & Xiaoping, W., 1992. Comparison of orientations of stress and strain tensor based on fault plane solutions in Kaoiki, Hawaii, *J. geophys. Res.,* **97,** 4769–4790.